

DETERMINATION OF POTENTIAL MULTI-TARGET INHIBITORS OF ALZHEIMER'S DISEASE *IN SILICO*

Massimo D. Bezoari†, Glendalyn Boothe\*

Northwestern State University, Louisiana Scholars' College, Natchitoches, LA 71497

## Abstract

The complexity of Alzheimer's disease requires therapeutic treatments that counteract multiple processes. Symptoms and causes include formation of senile plaques, agglomeration of neurofibrillary tangles, disruption of cholinergic activity, and oxidative stress. Enzymes that promote these pathways include BACE1, GSK-3 $\beta$ , CDK-5, AChE, BuChE, MAO-A, and MAO-B. Virtual screening of the InterBioScreen and Zinc 15 databases was conducted using the Schrödinger 2019 Phase program to identify potential inhibitors of these enzymes. InterBioScreen compounds 1N-05528, and 1N-72595, and Zinc 15 compounds ZINC314161, ZINC5854353, ZINC15674654, ZINC49170543, ZINC96112244, and ZINC604382088 all showed exergonic binding within the active sites of at least five AD enzymes. These compounds were docked individually with standard precision (SP) and compared with known inhibitors—the docking locations and scores were comparable with those of known inhibitors. ADME blood brain permeability evaluations with QPlogBB and QPMDCK showed that the compounds should not be blocked by the blood brain barrier.

†Corresponding author: bezoarim@nsula.edu

Keywords: Alzheimer's Disease, Multi-Target Directed Ligands, Schrödinger Virtual Screening, Maestro Docking, Pharmacophore Modeling, InterBioScreen, Zinc 15.

## Background

Alzheimer's disease (AD) is a neurodegenerative disease that affects 10% of people over the age of 65 and almost 50% over 85 (1, 2). AD is the leading cause of dementia and the sixth leading cause of death in the United States (3). The anticipated increasing numbers of AD cases requires more effective therapies than are currently available. Although several attempts have been made to explain the onset of the disease, its cause is still unclear (4, 5).

## Amyloid Cascade Hypothesis

According to the amyloid cascade hypothesis, the formation of senile plaques is the cause of AD (6). These aggregates of  $\beta$ -amyloid ( $\beta$ A) protein are formed on the outside of neurons of the brain, when amyloid precursor proteins (APPs) are hydrolyzed by secretases (7). Since 1992, one of the goals of AD research has been the inhibition of  $\beta$ -secretase, BACE1 (1, 8).

BACE1 can be inhibited at the active site where catalytic cleavage of substrate APP occurs. Binding of substrates or inhibitors at the active site causes a "flap" consisting of residues 69-75 to cover the site in a closed conformation or semi-closed conformation (9, 10). Thus, "Compound A" (Figure 1) is bound to the closed conformation of BACE1 in the Protein Data Bank (PDB) structure 2P4J. Compound A gave a  $K_i$  value of 1.1 nM for inhibition of BACE1 (11).  $K_i$  is a measure of binding affinity, i.e., the concentration of an inhibitor for which the inhibitory reaction rate is half its maximal rate. Values in the low nM range indicate very strong binding. It also showed an  $IC_{50}$  value of 39 nM according to a cellular inhibition assay.  $IC_{50}$  values measure the concentration of inhibitor required to reduce the rate of a biological process by half. The semi-closed conformation of BACE1 is complexed with "compound B" in the PDB structure 4H3G. Compound B (Figure 1) has shown a  $K_i$  value of 6 nM and an  $IC_{50}$  value of 48 nM (12). These downloaded PDB structure files were used in the present work, to screen databases and to determine which screened compounds would bind to BACE1 *in silico* in a similar manner.

## Tau Hypothesis

According to the tau hypothesis, AD is caused by tau protein that normally stabilizes microtubules and promotes self-assembly (13). Neurofibrillary tangles (NFTs) are formed through aggregation of tau protein caused by folding and insolubility due to hyperphosphorylation which changes the charges and conformations of the proteins (3, 14, 15). Two kinases that contribute to hyperphosphorylation are glycogen synthase kinase-3 $\beta$  (GSK-3 $\beta$ ) and cyclin-dependent kinase-5 (CDK-5). Inhibitors of GSK-3 $\beta$ , such as AR-A014418 (Figure 1) bind to the ATP binding site and prevent phosphorylation of tau (16, 17). AR-A014418 showed an  $IC_{50}$  value of 104 nM with values for other CDKs above 100  $\mu$ M (18).

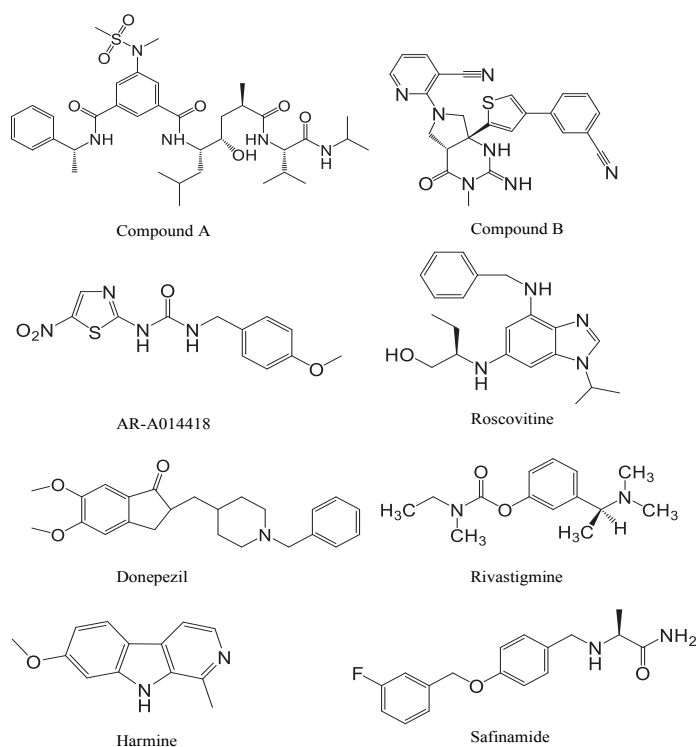


Figure 1. Known Inhibitors of AD Enzymes.

(R)-roscovitine is a CDK-1, CDK-2, and CDK-5 inhibitor that has been shown to inhibit CDK-5 with an  $IC_{50}$  value of 0.2  $\mu\text{M}$  (20). In the present work, the PDB files of AR-A014418 and roscovitine bound to GSK-3 $\beta$  (1Q5K) and CDK-5 (1UNL), respectively, were used for ligand screening.

### Cholinergic Hypothesis

The cholinergic hypothesis states that the cognitive decline of AD patients is due to abnormal function of cholinergic neurons, i.e., those that use the neurotransmitter, acetylcholine (ACh). AD patients experience a decline in both ACh receptor types (muscarinic and nicotinic) leading to decreased cholinergic activity (21). Inhibition of enzymes that are responsible for the breakdown of ACh, i.e., acetylcholinesterase (AChE) and butyrylcholinesterase (BuChE), may prevent decreases in cognitive function (3). AChE has greater specificity for ACh, while BuChE also hydrolyzes adippylcholine, succinylcholine, and benzoylcholine (22-24).

Four AChE inhibitor drugs are approved by the FDA for the treatment of AD: donepezil (Aricept®), rivastigmine (Exelon®), galantamine (Razadyne®), and memantine (Namenda®). All four reduce but do not halt cognitive decline symptoms (25). Donepezil and rivastigmine (Figure 1) have shown  $IC_{50}$  values for AChE of 6.7 nM and 4.3 nM, respectively. Rivastigmine also inhibits BuChE with an  $IC_{50}$  of 31 nM (26). In this work, the donepezil-AChE complex (4EY7) was used for screening of potential new ligands. The inhibitory properties of rivastigmine led us to carry out our own docking of that drug to human BuChE (2PM8), as a crystallographic analysis is not available for that complex.

### Oxidative Stress Hypothesis

According to the oxidative stress hypothesis, AD is caused by reactive oxygen species (ROS) that cause destruction of cholinergic neurons and formation of senile plaques. Reactive oxygen radicals can cause oxidation of RNA, DNA, proteins, and lipids (27). Monoamine oxidases (MAOs) catalyze primary amine deamination of major neurotransmitters and produce  $\text{H}_2\text{O}_2$ , promoting oxidative stress. MAO inhibitors improve cognitive function by relieving oxidative stress and neuroinflammation,

and regulating neurotransmitters (28). In the present work, the PDB files of MAO-A with harmine (2Z5X) and MAO-B with safinamide (2V5Z) were used for database screening. Harmine (Figure 1) has shown an  $IC_{50}$  value of 2-5 nM for MAO-A (29). Safinamide (Xadago®, Figure 1), an FDA-approved therapy for Parkinson's Disease, is a selective inhibitor of MAO-B with an  $IC_{50}$  value of 0.098  $\mu\text{M}$  (30, 31).

### Computational Strategies

One goal of the present work was to promote computational screening methods that might identify drug candidates for the treatment of AD. This would decrease the number, the time required, and the costs of unsuccessful drugs reaching and going through clinical trials (32).

Schrödinger's Phase program was used with the e-pharmacophore method to generate a *hypothesis* for potential ligands of each AD enzyme. A *hypothesis* is a 3-D group of molecular sites of a ligand that are deemed to be essential for favorable binding to that receptor. The sites are those that contribute to intermolecular attractions, such as lipophilic (London), hydrogen bonding, coulombic, polar and the like.

In a combined ligand-based virtual screening (LBVS) and structure-based virtual screening (SBVS) approach, the important binding sites for each enzyme are determined by optimizing the enzyme-known inhibitor PDB complex structure. Glide XP scoring evaluates which binding sites and interactions are the most important. Excluded volumes (regions of the pharmacophore that should not contain atoms) are defined. Further modifications can be made to the *hypothesis*: representation of hydrogen bonds as projected points instead of vectors relaxes the strictness of directionality of hydrogen bonding and permits a greater number of acceptable options in possible matches; feature matching tolerances, which are limits on distance ranges that the ligand features must be within to match the *hypothesis*, are selected. The *hypothesis* is used to screen databases for compounds with similar types and orientations of pharmacophore sites.

Database screening requires preparation: skipping ligand

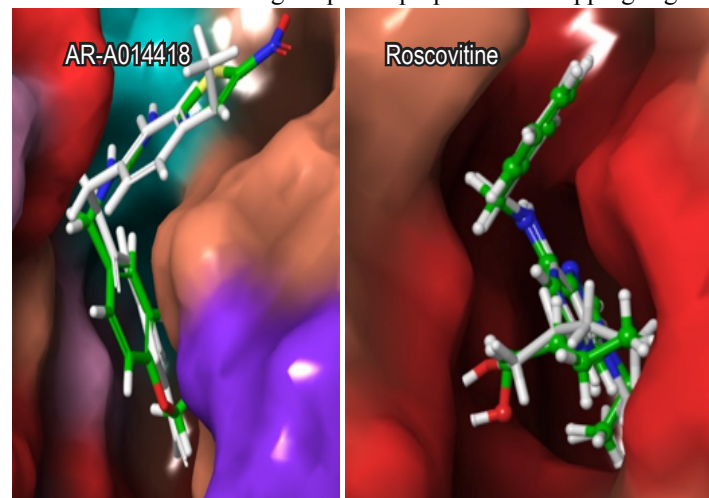
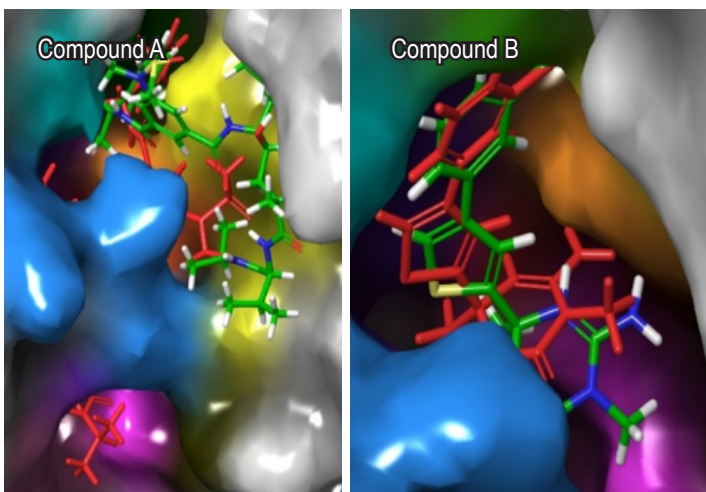


**Figure 3. Kinases GSK-3 $\beta$  and CDK-5 with Docked Known Inhibitors** Left: GSK-3 $\beta$  (from 1Q5K) with AR-A014418; right: CDK-5 (from 1UNL) with roscovitine. White structures: inhibitor pose in downloaded file; green-carbon structures: inhibitor docked after removal from complex and optimization of ligand-free protein.

**Figure 2. Secretases with Docked Known Inhibitors.** Left: BACE1 (closed conformation, from 2P4J) with "Compound A"; right: BACE1 semi-closed conformation (from 4H3G) with "Compound B.". Red structures: inhibitor pose in downloaded file; green-carbon structures: inhibitor docked after removal from complex and optimization of ligand-free protein.

duplicates; generating conformations; ligand optimization with Schrödinger's LigPrep; and prefiltering based on Lipinski's rule of five using the QikProp program (33, 34). Lipinski's rule of five "filters" the compounds using four rules with values that are multiples of five:  $\leq 5$  hydrogen bond donors,  $\leq 10$  hydrogen bond acceptors, a molecular mass that is  $< 500$  Da, and a partition coefficient ( $\log P$  value) that is  $\leq 5$  (35). QikProp predicts absorption, distribution, metabolism, and excretion (ADME) descriptors and pharmaceutical properties of organic molecules, comparing them to 95% of known drugs. The program calculates QPlogBB, the blood brain barrier (BBB) partition coefficient for orally delivered drugs. The QPPMDCK calculation predicts the permeability in nm/s of the Madin-Darby canine kidney (MDCK) epithelial cells, which mimic the BBB and are commonly used in research.

The Glide docking program calculates various parameters to evaluate and rank binding affinities of ligands and the preferred poses (36) using

$$\text{GlideScore} = 0.065E_{\text{vdw}} + 0.130E_{\text{Coul}} + E_{\text{Lipo}} + E_{\text{Hbond}} + E_{\text{Metal}} + E_{\text{BuryP}} + E_{\text{RotB}} + E_{\text{Site}}$$

in which  $E_{\text{vdw}}$  is the van der Waals energy,  $E_{\text{Coul}}$  is the coulombic energy,  $E_{\text{Lipo}}$  rewards hydrophobic (London) interactions,  $E_{\text{Hbond}}$  rewards hydrogen bonds,  $E_{\text{Metal}}$  is the metal binding term,  $E_{\text{BuryP}}$  penalizes internal polar groups in hydrophobic regions,  $E_{\text{RotB}}$  penalizes immobile rotatable bonds, and  $E_{\text{Site}}$  rewards polar interactions in the active site. DockingScore adds the Epik program state penalties to the GlideScore. These penalties adjust the single "best" 3-D structure to take account of ionizable groups and tautomers that contribute to the isomeric structures of a compound within a specified pH range (37).

DockingScores were used throughout this work to estimate binding affinities of ligands to receptor enzymes. This entails several assumptions that mostly relate to difficulties in accounting for solvation effects in the natural processes. The true binding energy ( $\Delta G_{\text{BE}}$ ) is given by

$$\Delta G_{\text{BE}} = G_{\text{complex}} - G_{\text{protein}} - G_{\text{ligand}}$$

The various terms include solvation effects and the enthalpies and

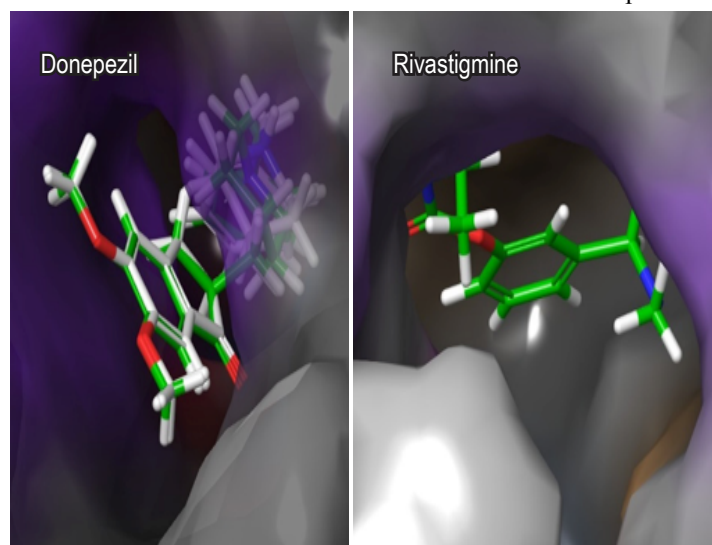


**Figure 4. Cholinesterases with Docked Known Inhibitors.** Left: AChE (from 4EY7) with donepezil; white structure, inhibitor pose in downloaded file; green-carbon structure, inhibitor docked after removal from complex and optimization of ligand-free protein. Right: BuChE (from 2PM8) with rivastigmine, docked in the present work.

entropies involved in the binding process. Even though some water molecules were retained in the docking procedures used in this work, such effects were assumed to be the same for the ligand-protein complexations occurring for a given enzyme. It is worth noting that the OPLS3e program used herein is an improvement over OPLS3, which is known to have a high degree of accuracy in predicting protein-ligand binding, with an RMS error of less than 1 kcal/mol when compared to measured binding affinities (38).

Related reports differ from the current study in that nearly all screenings were carried out for two enzymes only (39-41). Additionally, different databases, screening techniques, and computational software were used. Most of the studies used ligand-based virtual screening (LBVS); some used docking for screening instead of a pharmacophore, and some built quantitative structure-activity relationships (QSARs) models. The research that is closest to the present work screened for five of the eight enzymes used herein, omitting MAO-A and BuChE, and one BACE1 structure; multi-target inhibitors that inhibited only two or three of the enzymes were evaluated further; only the InterBioScreen 2016 database of ligands (63,409 compounds) was employed (41). In the present work, a higher standard (i.e., at least five favorable target enzyme DockingScores) was used; additionally, new versions of two databases, InterBioScreen (2019) and Zinc 15 (2015) were screened with 67,933 and 105,873 compounds, respectively (42, 43).

## Materials and Methods

Crystal structure analyses of the targets were obtained from the RCSB Protein Data Bank. The PDB IDs for the enzyme complexes were: 2P4J, human BACE1 closed conformation co-crystallized with "compound A;" 4H3G, human BACE1 semi-closed conformation with "compound B;" 1Q5K, human GSK-3 $\beta$  with ARA014418; 1UNL, human CDK-5 with roscovitine; 4EY7, human AChE with donepezil; 2PM8, human BuChE with no ligand—rivastigmine was docked to the enzyme in the present work; 2Z5X, human Monoamine Oxidase A with harmine; and 2V5Z, human Monoamine Oxidase B with safinamide.

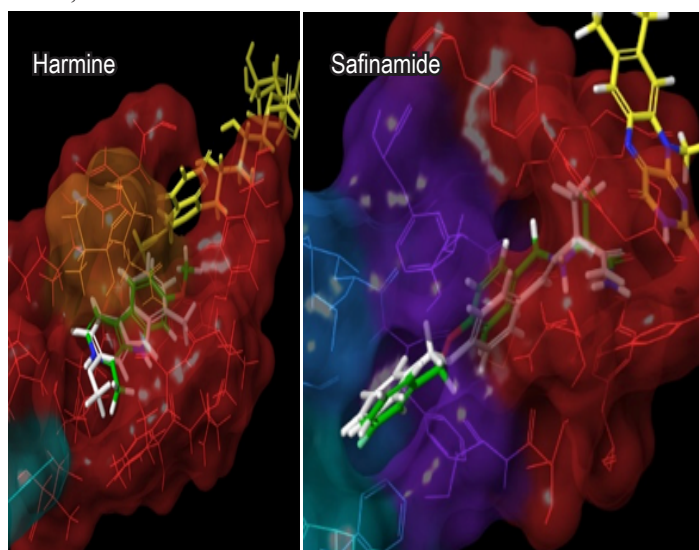


**Figure 5. MAO Active Sites with Docked Known Inhibitors Harmine and Safinamide.** Left: MAO-A (from 2Z5X); right: MAO-B (from 2V5Z). White structures: inhibitor pose in downloaded file; green carbon structures: inhibitor docked after removal from complex and optimization of ligand-free protein. Yellow structures: FAD co-factor.

### Phase e-Pharmacophore Hypothesis and Database Screening

Each e-pharmacophore hypothesis was created using Phase with excluded volumes. If four or more pharmacophore sites were obtained, they were included in the pharmacophore hypothesis only if the XP scores for the interactions were more exergonic than -0.4 kcal/mol; for hypotheses with less than four sites, all were retained. Hydrogen bond donors were set as projected points. Default settings were used for feature distances (RMSD = 2 Å for different feature types, 4.00 Å for the same feature type). Ligands prepared from the downloaded databases were screened using the hypotheses generated for the individual enzymes.

The natural products database was downloaded from InterBioScreen (42). The Zinc 15 databases were: Analyticon Discovery Natural Derivatives, Analyticon Discovery NP, Analyticon Discovery NP BB, Aster Sunflower Family NP, AfroDb Natural Products, BIOFACQUIM, Biopurify Phytochemicals, Herbal Ingredients In-Vivo Metabolism, Herbal Ingredients Targets, HMBD Toxin, Indofine Natural Products, MolPort Natural Products (biogenic and metabolite subsets only), NPACT Database, Specs Natural Products, TCM Database @Taiwan (biogenic and metabolite subsets only), TimTec Natural Derivatives, and UEFS Natural Products (43). Each database was prepared with Schrödinger's Phase program—up to 50 conformers were generated for each ligand, which were prepared as follows: ionization states (using Epik) at pH 7.0,  $\pm$  2.0, selected; at most, one low-energy 5- or 6-membered ring conformation, selected; four low-energy stereoisomers for each ligand, retained; high-energy ionization states and tautomer states, removed. The ligands were “filtered” by Lipinski's Rule of Five using QikProp properties.

### High Throughput Virtual Screening (HTVS)

The output ligands from Phase screening were used to dock the ligands into their respective proteins using high-throughput virtual screening (HTVS), keeping the top 30% of the best compounds. Ligands with the most favorable binding scores for the active sites that also bound to the most proteins were selected for further SBVS docking analyses.

### Enzyme Docking Preparation

All polypeptide chains were kept for each enzyme except 2P4J for which chains B and C of the tetramer were deleted. Each protein receptor was prepared using the Protein Prep Wizard: ligands, crystallization solvents and non-enzyme metals, deleted; original hydrogens, deleted; new hydrogens, missing side chains and missing loops, added; bond orders, assigned; het groups (pH 7  $\pm$  2), added; water molecules beyond 5 Å from het groups, deleted; zero-order bonds to enzyme metals and disulfide bonds, created; waters, optimized; waters with less than 3 hydrogen bonds to non-waters, removed; structure using the OPLS3e force field, optimized.

### Enzyme Gridboxes

Small gridboxes were used for hypothesis creation and HTVS, and large gridboxes for the individual dockings of known inhibitors and selected ligands. Gridboxes for enzymes were prepared as follows: van der Waals scaling, none; aromatic H as donor hydrogen bonds and halogens as acceptors, included. The inner box, within which the midpoint of the docked ligand must lie, was centered on the active site of each enzyme; for small gridboxes, the

dimensions of the inner box were 10 Å x 10 Å x 10 Å, and for large gridboxes, 40 Å x 40 Å x 40 Å. The dimensions of the outer box, within which the entire ligand must lie, were determined by addition to the inner box of more than half the maximum length of the ligand; for small gridboxes this resulted in a box of about 40 Å x 40 Å x 40 Å, and for large gridboxes, about 70 Å x 70 Å x 70 Å.

### Protein-Ligand Complex Redocking

Known inhibitors and the ligands obtained from HTVS were docked to the enzymes using the following settings: scaling of van der Waals' radii, factor = 0.80 with partial charge cutoff = 0.15; precision = standard precision; ligand sampling = flexible; nitrogen inversions, sampled; ring conformations, sampled; biased sampling of torsions for all predefined functional groups, selected; Epik state penalties to DockingScores, added; aromatic H as hydrogen bond donors and halogens as acceptors, included; best poses reported, limited to 20; post-docking minimization, performed.

### QikProp

QikProp was run to find the QPlogBB and QPPMDCK values of the screened inhibitors.

## Results and Discussion

The pharmacophore hypotheses that were generated for each enzyme are summarized in Table 1. HTVS screening of the databases for matching ligands yielded 24 compounds from the InterBioScreen and 20 compounds from the Zinc 15 databases (Tables 2,3).

Tables 2 and 3 list the best pose Docking Scores within the active sites. For the most part, only the best five or six poses were examined which tended to be within 3 kcal/mol of the best score. A simplified analysis using the relationship

$$\Delta G_{BE} = -RT \ln K$$

in which K is the ratio of one ligand-receptor complex to a different one (for the same ligand and receptor), shows that a difference of 3 kcal/mol indicates a preference for the more exergonic pose of about 160-fold, so less exergonic poses were not considered.

Two compounds from InterBioScreen (1N05528 and 1N-72595) and six from Zinc 15 (ZINC314161, ZINC5854353, ZINC15674654, ZINC49170543, ZINC96112244, ZINC604382088) were selected for comparison to known inhibitors of AD enzymes. The selection was based on the HTVS determinations, based on DockingScores, that they might inhibit five or more AD pathway enzymes.

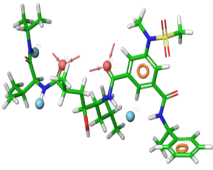
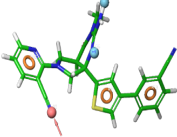
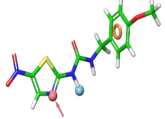
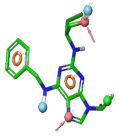
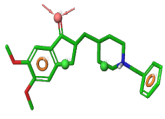
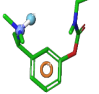
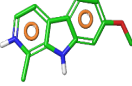
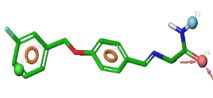
Docking analyses of most of the known inhibitors to these AD enzymes have not been reported previously. The results obtained demonstrated the integrity of the docking method. In each case, after deletion of the known inhibitor from the downloaded complex and optimization of the inhibitor-free enzyme, the inhibitors were docked to the enzyme to see if they would favor the active site. In every case—using large gridboxes that encompassed almost the entire subunit in question—the known inhibitor was shown to dock favorably within the active site of the enzyme it is known to inhibit. Typical results are illustrated in Figures 2-5.

In general, for each AD enzyme the most favorable DockingScores were obtained for the known inhibitor of that enzyme (Table 4). There were exceptions. “Compound A,” the known inhibitor of BACE1, showed more favorable binding to BuChE (-8.36 kcal/mol) than to BACE1 (2P4J, -7.21 kcal/mol). AR-A014418, the known inhibitor of GSK-3 $\beta$ , showed favorable binding to that enzyme (1Q5K, -6.71 kcal/mol), but “Compound B” gave a more exergonic value (-8.67 kcal/mol) that was beyond the RMS error of 1 kcal/mol. Experimental inhibition of GSK-3 $\beta$  by “Compound B” has not been reported, so it is possible that it is an inhibitor of GSK-3 $\beta$ . The exceptionally exergonic DockingScore of -10.47 kcal/mol corroborates experimental reports of roscovitine’s ability to inhibit CDK-5 (45). Although complexed structures for rivastigmine are not available, it is a recognized inhibitor of cholinesterases (26)—our docking results showed only moderate binding to AChE (4EY7, -6.02 kcal/mol) that was far less favorable than that of the other known inhibitor, donepezil (-13.38 kcal/mol) and even weaker binding to BuChE (2PM8, -4.79 kcal/mol). This does not negate the computational docking approach, as rivastigmine’s recognized anticholinesterase activity is due to covalent bonding within the active site shifting

the initial equilibrium of complexation to the product side (44). (Covalent docking was not sampled in the present work).

It is interesting to note that the monoamine oxidases seem to resist binding of compounds within the active site. No binding was observed within the active site of MAO-A (2Z5X) for any compound other than strongly exergonic binding of the known inhibitor, harmine (-9.96 kcal/mol). Moderate binding within the MAO-B (2V5Z) binding site was observed for “Compound B,” AR-A014418, and rivastigmine, in addition to the recognized inhibitor of MAO-A, harmine, that gave a strong exergonic

**Table 1. Pharmacophore Hypotheses.** A, acceptor (red spheres); D, donor (light-blue sphere); hydrophobic region (green sphere); P, positive ion (blue sphere); R, ring (orange circle).

Inhibitor	Sites (XP Score)	Model
Compound A	A6 (-0.47), A7 (-1.18) D9 (-0.70), D11 (-0.43), D12 (-0.70) R17 (-1.31), R18 (-0.94)	
Compound B	A2 (-1.00) D5 (-0.64), D7 (-0.71) R9 (-0.57), R10 (-0.64), R11 (-0.64)	
AR-A014418	A1 (-1.52) D4 (-2.18) R8 (-0.84)	
Roscovitine	A2 (-2.10) D5 (-0.62), D7 (-2.12) R11 (-0.75), R12 (-0.83)	
Donepezil	A3 (-1.68) H7 (-1.20), H8 (-1.96) R10 (-1.28), R11 (-1.45)	
Rivastigmine	D3 (-0.42) P5 (-0.27) R6 (-1.25)	
Harmine	R6 (-1.14), R7 (-1.18)	
Safinamide	A3 (-0.70) H6 (-0.30) R7 (-1.80), R8 (-1.37)	

**Table 2. DockingScore<sup>a</sup> Energies (kcal/mol) of InterBioScreen STOCK1N Compounds<sup>b</sup> to AD Enzymes from HTVS Screening.**

Title	BACE1 (2P4J)	BACE1 (4H3G)	GSK-3 $\beta$ (1Q5K)	CDK-5 (1UNL)	AChE (4EY7)	BuChE (2PM8)	MAO-A (2Z5X)	MAO-B (2V5Z)
1N-03766			-8.12	-8.99			8.53	
<b>1N-05528<sup>c</sup></b>	<b>-8.67</b>	<b>-7.18</b>	<b>-7.94</b>	<b>-7.31</b>		<b>-7.94</b>		
1N-05989				-8.93			-9.26	-7.31
1N-06592		-7.64		-6.34		-6.29		
1N-07221		-7.54	-6.90					-10.39
1N-11998		-6.03	-8.19		-12.03	-7.14		
1N-14475		-7.02				-6.74	-9.87	
1N-19625		-6.35			-12.62	-6.70		-9.15
1N-30985					-10.39		-9.63	-9.25
1N-31555			-8.37	-8.45				-9.07
1N-48784						-8.02	-9.50	
1N-55783			-8.95	-9.00			-7.09	
1N-70124			-6.99	-8.85			-9.64	
<b>1N-72595<sup>c</sup></b>		<b>-6.55</b>	<b>-6.66</b>	<b>-9.00</b>	<b>-11.12</b>			<b>-9.16</b>
1N-74248		-6.99	-7.18	-9.52				
1N-74528		-8.26	-6.17					-10.318
1N-77743	-4.60	-7.83		-6.34				
1N-81601	-7.93	-7.07	-7.17					
1N-82268		-6.97	-7.08	-7.29			-9.78	
1N-82334			-7.18	-6.68			-9.67	-9.66
1N-93603		-7.07	-6.64		-10.41	-8.29		
1N-94295		-6.222			-12.65	-7.52		
1N-94765		-6.26		-6.86	-12.83	-7.02		
1N-95043			-6.48	-9.37				-9.86

a. All values are from HTVS screening, using small grid boxes. Bolded values emphasize ligands which showed favorable docking to at least five enzymes.

b. InterBioScreen compound designations include the STOCK category, e.g. STOCK1N-05228.

c. Compounds blocking active sites of five or more enzymes are indicated in bold.

**Table 3. DockingScore Energies (kcal/mol) of Screened Inhibitors from Zinc15 Bound to AD Enzymes from HTVS Screening.**

Compound ID	BACE1 (2P4J)	BACE1 (4H3G)	GSK-3 $\beta$ (1Q5K)	CDK-5 (1UNL)	AChE (4EY7)	BuChE (2PM8)	MAO-A (2Z5X)	MAO-B (2V5Z)
ZINC39103		-7.79	-7.84	-7.43			-7.43	
<b>ZINC314161</b>		<b>-6.11</b>	<b>-8.42</b>	<b>-7.87</b>			<b>-7.93</b>	<b>-9.33</b>
ZINC1663391		-7.48	-6.06	-7.48			-8.59	
ZINC3881190		-6.25	-6.40	-8.05			-10.05	
ZINC4024311		-7.883				-7.36		-9.54
<b>ZINC5854353</b>	<b>-7.12</b>	<b>-7.50</b>	<b>-6.46</b>	<b>-7.08</b>				<b>-7.81</b>
ZINC8733315		-6.48	-6.99	-8.85			-9.64	
<b>ZINC15674654</b>	<b>-5.56</b>	<b>-7.60</b>	<b>-5.63</b>	<b>-6.71</b>		<b>-7.26</b>		
ZINC15675012	-7.44	-6.79		-6.60				-9.46
ZINC20503251		-7.64		-6.11	9.30	-6.49		
ZINC33376662		-7.73	-6.26	-6.77				-9.37
ZINC35446702			-8.26	-8.10		-7.00		-9.46
<b>ZINC49170543</b>	<b>-6.73</b>	<b>-5.94</b>	<b>-5.30</b>	<b>-7.44</b>	<b>-12.20</b>			<b>-7.60</b>
ZINC82383995			-8.12	-7.73			-9.65	
<b>ZINC96112244</b>	<b>-7.73</b>		<b>-5.79</b>		<b>-8.94</b>	<b>-6.31</b>		<b>-8.94</b>
ZINC96112282		-6.15	-7.28		-12.32			
ZINC209522569		-8.105		-6.71	-6.18			
ZINC253406919		-7.61				-6.70		
<b>ZINC604382088</b>	<b>-8.50</b>	<b>-6.15</b>	<b>-5.77</b>	<b>-7.28</b>		<b>-6.91</b>		

a. All values are from HTVS screening, using small grid boxes. Bolded values emphasize ligands which showed favorable docking to at least five enzymes.

b. Complete Zinc-15 compound designations include the prefix “Zinc,” e.g., ZINC15674654.

c. Compounds blocking active sites of five or more enzymes are indicated in bold. These were selected for individual analyses.

DockingScore of -8.20 kcal/mol. Harmine also demonstrated very favorable binding to AChE (-9.98 kcal/mol)—a result that corroborates reported strong inhibition of AChE by harmine and which reinforces the validity of the *in silico* docking approaches herein (46). Safinamide, a known inhibitor of MAO-B (30, 31), demonstrated a very favorable binding interaction within the active site of MAO-B (-10.54 kcal/mol), as well as to AChE (-10.35 kcal/mol). Although safinamide has not been used for AD therapy, it may be an effective cholinesterase inhibitor.

Individual docking results for the compounds selected from HTVS screening to AD enzymes are shown in Table 5. Relating to potential inhibition of the amyloid pathway in AD, two ligands, 1N-05528 and ZINC604382088, bound more exergonically (-8.76 kcal/mol and -8.25 kcal/mol, respectively) to closed conformation BACE 1 (2P4J) than the recognized inhibitor “Compound A” (-7.21 kcal/mol). The improvement exceeded the RMS error of 1 kcal/mol. Two others, ZINC96112244 (-7.02 kcal/mol) and ZINC314161 (-6.46 kcal/mol), were within 1 kcal/mol of “Compound A.” None of the ligands bound to the semi-closed BACE1 (43HG) as strongly as the known inhibitor “Compound B” (-8.96 kcal/mol). However, all eight ligands showed moderate to strong binding (-6.2 to -7.8 kcal/mol).

Compound ID	BACE1 (2P4J)	BACE1 (4H3G)	GSK-3 $\beta$ (1Q5K)	CDK-5 (1UNL)	AChE (4EY7)	BuChE (2PM8)	MAO-A (2Z5X)	MAO-B (2V5Z)
<b>Compound A</b>	<b>-7.21</b>	-6.47	-6.51 <sup>b</sup>	-5.70 <sup>c</sup>	None	-8.36 <sup>d</sup>	None	None
<b>Compound B</b>	-5.32 <sup>d</sup>	<b>-8.96</b>	-8.67	-6.46 <sup>c</sup>	-6.54 <sup>b</sup>	-7.91	None	-5.80 <sup>e</sup>
<b>AR-A014418</b>	-5.62	-5.25	<b>-6.71</b>	-7.23 <sup>c</sup>	-6.54	-5.69	None <sup>f</sup>	-6.34 <sup>e</sup>
<b>Roscovitine</b>	-5.15	-5.72	5.45 <sup>g</sup>	<b>-10.47</b>	-5.29	-6.40	None	None <sup>c</sup>
<b>Donepezil</b>	-6.09	-6.93	-6.23 <sup>a</sup>	-6.39	<b>-13.38</b>	-7.75	None <sup>c</sup>	None <sup>c</sup>
<b>Rivastigmine</b>	-4.02	-3.53	None <sup>f</sup>	-6.96	<b>-6.02</b>	<b>-4.79</b>	None <sup>f</sup>	-6.051
<b>Harmine</b>	-6.22	-6.79 <sup>c</sup>	-6.91 <sup>b</sup>	-6.48	-9.98	-5.34	<b>-9.96</b>	-8.20
<b>Safinamide</b>	-7.37	-6.26	-7.74	-7.46	-10.35	-6.32	None	<b>-10.54</b>

a. Scores of the known inhibitor complexes are indicated in bold red.

b. The best poses were partially within the active sites Other poses were remote.

c. Top poses within the active site. Others were adjacent and/or remote.

d. From best pose. Some poses within active site, but most were remote.

e. Poses were at the active site but not within.

f. Some poses adjacent to active site.

g. From sixth best pose. Top poses were not within active site.

For possible inhibition of AD tauopathy pathways, all the ligands bound to GSK-3 $\beta$  with binding energies in the range -6.12 to -7.68 kcal/mol, equivalent to the known inhibitor AR-A014418 (-6.71 kcal/mol). In the present work, roscovitine exhibited a strongly favorable DockingScore to CDK-5 (1UNL) of -10.47 kcal/mol. Although none of the screened ligand complexations were as exergonic as this, all were moderate to strong binders to CDK-5, with scores ranging between -6.84 and -9.41 kcal/mol.

Relating to possible inhibition of the cholinergic AD pathways, although none of the ligands bound as strongly to AChE (4EY7) as donepezil (-13.38 kcal/mol), all showed stronger binding (-8.72 to -10.65 kcal/mol) than the other known acetylcholinesterase inhibitor, rivastigmine (-6.02 kcal/mol). Similarly, all the ligands showed equivalent or more favorable DockingScores (-5.70 to -9.07 kcal/mol) to BuChE (2PM8) than rivastigmine (-4.79 kcal/mol). However, as stated previously, final rivastigmine binding is covalent.

For possible inhibition of the oxidative stress AD pathway, five ligands, 1N-05528, ZINC96112244, ZINC15674654, ZINC49170543, and ZINC05854353 showed moderate DockingScores to MAO-A (2Z5X) of -5.6 to -6.51 kcal/mol that

Compound ID	BACE1 (2P4J)	BACE1 (4H3G)	GSK-3 $\beta$ (1Q5K)	CDK-5 (1UNL)	AChE (4EY7)	BuChE (2PM8)	MAO-A (2Z5X)	MAO-B (2V5Z)
<b>1N-05528</b>	-8.76	-7.28	-7.28	-8.94	-8.72 <sup>a</sup>	-8.22	-6.00 <sup>c</sup>	-8.36 <sup>b</sup>
<b>1N-72595</b>	-6.05	-6.49	-6.78 <sup>b</sup>	-9.41	-9.40	-8.42	None	-8.96 <sup>c</sup>
<b>ZINC314161</b>	-6.17	-6.59	-7.14 <sup>a</sup>	-8.02	-9.44	-5.70 <sup>c</sup>	None	-10.14
<b>ZINC5854353</b>	-6.03	-7.80	-7.46	-7.72	-9.39	-7.11	-6.17 <sup>d</sup>	-8.70 <sup>a</sup>
<b>ZINC15674654</b>	-6.46	-7.60	-6.12 <sup>a</sup>	-7.72	-9.70	-8.38	-6.07 <sup>d</sup>	-7.47 <sup>c</sup>
<b>ZINC49170543</b>	-6.16	-7.05	-7.28	-7.44	-12.24	-8.48	-6.51 <sup>a</sup>	-7.45 <sup>c</sup>
<b>ZINC96112244</b>	-7.02	-6.20	-6.36	-6.84 <sup>a</sup>	-10.65	-7.70	-5.60 <sup>d</sup>	-8.17 <sup>a</sup>
<b>ZINC604382088</b>	-8.25	-7.78	-7.68	-8.71 <sup>a</sup>	-10.43	-9.07	None	-9.38 <sup>a</sup>

a. From the most exergonic pose. Other poses were observed adjacent to and/or remote from the active site.

b. From the 2<sup>nd</sup> most exergonic pose. Other poses were observed adjacent to the active site.

c. All poses adjacent to the active site.

d. All poses only partially blocked the active site or were remote.

e. From the 4<sup>th</sup> most exergonic pose. Most poses were remote from the active site.

were below the strongly exergonic binding of the known inhibitor harmine (-9.96 kcal/mol). All the ligands showed moderate to strong binding to MAO-B (2V5Z) with DockingScores of -7.45 to -10.14 kcal/mol that were less favorable or equivalent to the safinamide score of -10.54 kcal/mol.

All the ligands selected from the screening process in this work had blood brain barrier permeability properties, indicated by QPlogBB and QPPMDCK, in the recommended range -3.0 to 1.2 for QPlogBB, and 25 to 500 or better for QPPMDCK (Table 6).

## Conclusions

Multi-target directed ligands (MTDLs) may have significant advantages over other drugs in clinical trials or FDA-approved drugs for the treatment of AD. The potential therapeutic improvements are augmented in light of recent advances in detecting AD at an early stage of the disease (47), because treatment by a single multi-target ligand at initial stages might significantly decrease the rate of disease progression.

HTVS screening identified 24 InterBioScreen compounds and 20 from Zinc 15 as having potential therapeutic properties against processes that relate to AD. Eight ligands (1N-05528, 1N-72595, ZINC314161, ZINC5854353, ZINC15674654, ZINC49170543, ZINC96112244, ZINC604382088) were analyzed further through SP docking studies. The results showed binding affinities, as measured by DockingScores, that were comparable to known inhibitors of enzymes that promote AD and/or AD symptoms (Table 5). This indicates promising potential for being able to function as multi-target directed ligands (MTDLs). Some of the known inhibitors of at least one AD pathway enzyme also showed binding to multiple enzymes, namely, donepezil, harmine, and safinamide. For example, the FDA-approved anticholinesterase drug, donepezil, indicates moderate binding to BACE, as well as the kinases

GSK-3 $\beta$  and CDK-5. In fact, inhibition of BACE by donepezil has been reported (48, 49).

Docking of all original inhibitors (obtained from co-crystallized PDB structures, after deletion of the inhibitor and optimization of the ligand-free enzyme), and of the ligands found by HTVS screening showed complexation within the active sites with poses similar to those in the original PDB structures. This indicates that the pharmacophore screening and HTVS docking procedures were reliable for finding compounds with chemical properties that mimic the original inhibitors.

Although this work pursued detailed studies for ligands that showed potential to inhibit 5 or more AD enzymes, other compounds in Tables 2 and 3 showed favorable docking to two or more enzymes, and might be worth studying either as MTDLs, or as compounds that could serve as base structures for suitable synthetic analogs. It is worth noting that four of the 44 ligands found are natural products. ZINC05854353, or luteone, is present in common beans; ZINC1663391, can be found in *Muscari comosum*, also known as the tassel hyacinth; STOCK1N-05989, or naringenin, is a flavonoid often found in citrus fruits, tomatoes, and figs; STOCK1N-74248, or sulfuretin, is a flavonoid isolated from *Toxicodendron vernicifluum*, also known as the Chinese lacquer tree.

Limitations of this study include: reliance on solid state crystallographic structures based on solids that can only be obtained after treatments with solvents, salt solutions, and solutions of varying pH that may cause structural changes in proteins and complexes; possible differences between the solvated protein-ligand complexes and the isolated computational structures; the docking of one ligand to one receptor (neglect of multi-drug complexation effects); and flexibility constraints of protein receptors.

This research illustrates a valid approach for rapid screening of suitable drug candidates and promotes the discovery of novel compounds, including natural products, for the advancement of therapeutic treatments for Alzheimer's disease. This work could be continued through expanded docking studies and compound selections, and laboratory enzymatic assays of compounds to analyze their inhibitory effects.

## Acknowledgements

The authors gratefully acknowledge support of this work from the Richard Lounsbery Foundation, in the form of a Research Professorship to Massimo D. Bezoari, and from Northwestern State University, in the form of a Jove Scholarship to Glendalyn Boothe.

## References

- Mattson, M. P.; Duan, W.; Pedersen, W. A.; Culmsee, C. *Apoptosis* **2001**, *6*, 69-81.
- Lee, S. C.; Nam, E.; Lee, H. J.; Savelieff, M. G.; Lim, M. H. *Chem. Soc. Rev.* **2017**, *2*, 310-323.
- Kumar, A.; Kumar, A. Alzheimer's Disease Molecules: Present and Future Molecules. In *Computational Modeling of Drugs Against Alzheimer's Disease*. Kunal Roy, Ed.; Neuromethods 132; Springer Nature: New York, NY, 2018; pp 3-22.
- Du, X.; Wang, X.; Geng, M. *Transl. Neurodegener.* **2018**, *7*, 1-7.
- Alzheimer's Association. Facts and Figures. 2019a. <https://www.alz.org/alzheimers-dementia/facts-figures> (accessed Apr 2,

**Table 6. Blood Brain Barrier Permeability Properties of All Ligands.**

Ligand	QPlogBB	QPPMDCK
Compound A	-2.868	58.732
Compound B	-2.040	32.598
AR-A014418	-1.431	145.466
Roscovitine	-0.734	1112.997
Donepezil	0.100	476.934
Rivastigmine	-1.661	75.694
Harmine	0.194	2496.985
Safinamide	-0.408	228.474
1N-05528	-0.588	74.845
1N-72595	-1.001	222.573
ZINC314161	-1.331	91.258
ZINC5854353	-1.661	75.694
ZINC15674654	-0.589	63.114
ZINC49170543	-0.189	155.638
ZINC96112244	0.408	1476.331
ZINC604382088	-0.532	35.415

2019).

6. Scotti, L.; Scotti, M. T. In Silico Studies Applied to Natural Products with Potential Activity. In *Computational Modeling of Drugs Against Alzheimer's Disease*. Kunal Roy, Ed.; Neuromethods 132; Springer Nature: New York, NY, 2018; pp 513-531.
7. Armstrong, R. A. *Folia Neuropathol.* **2009**, 47(4), 289-299.
8. Koelsch, G. *Molecules* **2017**, 22.
9. Shimizu, H.; Tosake, A.; Kaneko, K.; Hisano, T.; Sakurai, T.; Nukina, N. *Mol. Cell. Biol.* **2008**, 28 (11), 3663-3671. <https://www.ncbi.nlm.nih.gov/pubmed/articles/PMC2423307/> (accessed Oct 14, 2019).
10. Das, S.; Chakraborty, S.; Basu, S. *Sci. Rep.* **2019**, 9(1), 3714.
11. Ghosh, A. K.; Kumaragurubaran, N.; Hong, L.; Kulkarni, S. S.; Xu, X.; Chang, W.; Weerasena, V.; Turner, R.; Koelsch, G.; Bilcer, G.; Tang, J. *J. Med. Chem.* **2007**, 50, 2399-2407. <https://pubs.acs.org/doi/10.1021/jm061338s> (accessed Oct 14, 2019).
12. Mandal, M.; Zhu, Z.; Cumming, J. N.; Liu, X.; Strickland, C.; Mazzola, R. D.; Caldwell, J. P.; Leach, P.; Grzelak, M.; Hyde, L.; Zhang, Q.; Terracina, G.; Zhang, L.; Chen, X.; Kuvelkar, R.; Kennedy, M. E.; Favreau, L.; Cox, K.; Orth, P.; Buevich, A.; Voigt, J.; Wang, H.; Kazakevich, I.; McKittrick, B. A. Greenlee, W.; Parker, E. M. Stamford, A. W. *J. Med. Chem.* **2012**, 55, 9331-9345.
13. Kametani, F.; Hasegawa, M. *Front. Neurosci.* **2018**, 12, 1-11.
14. Mandelkow, E.; Mandelkow, E. *Cold Spring Harbor Perspect. Med.* **2012**, 2, 1-25.
15. Alonso, A. D.; Cohen, L. S.; Corbo, C.; Morozova, V.; Elldrissi, A.; Phillips, G.; Kleiman, F. E. *Front. Cell. Neurosci.* **2018**, 12, 1-11.
16. Gomez-Ganau, S.; deJulian-Ortiz, J. V.; Gozalbes, R. Recent Advances in Computational Approaches for Designing Potential Anti-Alzheimer's Agents. In *Computational Modeling of Drugs Against Alzheimer's Disease*. Kunal Roy, Ed.; Neuromethods 132; Springer Nature: New York, NY, 2018; pp 25-59.
17. Eldar-Finkelman, H.; Martinez, A. *Front. Mol. Neuro.* **2011**, 4, 1-18.
18. Shukla, V.; Skuntz, S.; Pant, H. C. *Arch. Med. Res.* **2012**, 43(8), 655-662.
19. Mapelli, M.; Massimiliano, L.; Crovace, C.; Seeliger, M. A.; Tsai, L.; Meijer, L.; Musacchio, A. *J. Med. Chem.* **2005**, 48, 671-679.
20. Meijer, L.; Borgne, A.; Mulner, O.; Chong, J. P.; Blow, J. J.; Inagaki, N.; Inagaki, M.; Delcros, J.; Moulinoux, J. *Eur. J. Biochem.* **1997**, 243, 527-536.
21. Hampel, H.; Mesulam, M.; Cuello, A. C.; Farlow, M. R.; Giacobini, E.; Grossberg, G. T.; Khachaturian, A. S.; Vergallo, A.; Cavedo, E.; Snyder, P. J.; Khachaturian, Z. S. *Brain* **2018**, 141(7), 1917-1933.
22. Pang, X.; Fu, H.; Yang, S.; Wang, L.; Liu, A.; Wu, S.; Du, G. *Molecules* **2017**, 22, 1-15.
23. Zlatkovic, M.; Krstic, N.; Subota, V.; Boskovic, B.; Vucinic, S. *Vojnosanit. Pregl.* **2017**, 74(8), 736-741.
24. Gupta, S.; Mohan, C. G. *BioMed Res. Int.* **2014**, 2014, 1-21.
25. Alzheimer's Association. Medications for Memory. 2019b. <https://www.alz.org/alzheimers-dementia/treatments/medications-for-memory> (accessed Apr 2, 2019).
26. Ogura, H.; Kosasa, T.; Kuriya, Y.; Yamanishi, Y. *Methods Find. Exp. Clin. Pharmacol.* **2000**, 22(8), 609-613.
27. Gandhi, S.; Abramov, A. Y.; *Oxid. Med. Cell. Longevity* **2012**, 2012(3), 1-11.
28. Cai, Z. *Mol. Med. Rep.* **2014**, 9, 1533-1541.
29. Brierley, D.; Davidson, C. *Prog. Neuro-Psychopharmacol. Biol. Psychiatry* **2012**, 39, 263-272. <https://www.ncbi.nlm.nih.gov/pubmed/22691716> (accessed Oct 9, 2019).
30. Finberg, J. P.; Rabey, J. M. *Front. Pharmacol.* **2016**, 7, 1-16. <https://www.ncbi.nlm.nih.gov/pmc/articles/PMC5067815/> (accessed Oct 9, 2019).
31. Binda, C.; Wang, J.; Pisani, L.; Caccia, C.; Carotti, A.; Salvati, P.; Edmondson, D. E.; Mattevi, A. *J. Med. Chem.* **2007**, 50, 5848-5852. <https://pubs.acs.org/doi/10.1021/jm070677y> (accessed Oct 9, 2019).
32. Leelananda, S. P.; Lindert, S. *Beilstein J. Org. Chem.* **2016**, 12, 2694-2718. <https://www.ncbi.nlm.nih.gov/pubmed/28144341> (accessed Oct 8, 2019).
33. **Schrödinger Release 2019-1**: Phase, Schrödinger, LLC, New York, NY, 2019.
34. **Schrödinger Release 2019-3**: QikProp, Schrödinger, LLC, New York, NY, 2019.
35. Awasthi, M.; Singh, S.; Tiwari, S.; Pandey, V. P.; Dwivedi, U. N. Computational Approaches for Therapeutic Application of Natural Products in Alzheimer's Disease; In *Computational Modeling of Drugs Against Alzheimer's Disease*. Kunal Roy, Ed.; Neuromethods 132; Springer Nature: New York, NY, 2018; pp 483-511.
36. **Schrödinger Release 2019-3**: Glide, Schrödinger, LLC, New York, NY, 2019.
37. **Schrödinger Release 2019-3**: Epik, Schrödinger, LLC, New York, NY, 2019.
38. Harder, E.; Damm, W.; Maple, J.; Wu, C.; Reboul, M.; Xiang, J. Y.; Wang, L.; Lupyan, D.; Dahlgren, M. K.; Knight, J. L.; Kaus, J. W.; Cerutti, D. S.; Krilov, G.; Jorgensen, W. L.; Abel, R.; Friesner, R. A. *J. Chem. Theory Comput.* **2016**, 12, 281-296. <https://pubs.acs.org/doi/10.1021/acs.jctc.5b00864> (accessed Mar 2019).
39. Basile, L. Virtual Screening in the Search of New and Potent Anti-Alzheimer Agents. In *Computational Modeling of Drugs Against Alzheimer's Disease*. Kunal Roy, Ed.; Neuromethods 132; Springer Nature: New York, NY, 2018; pp 107-137.
40. Chen, Y.; Lin, H.; Yang, H.; Tan, R.; Bian, Y.; Fu, T.; Li, W.; Wu, L.; Pei, Y.; Sun, H. *RSC Adv.* **2017**, 7, 3429-3438. <https://pubs.rsc.org/en/content/articlepdf/2017/ra/c6ra25887e> (accessed Oct 8, 2019).
41. Ambure, P.; Bhat, J.; Puzyn, T.; Roy, K. *J. Biomol. Struct. Dyn.* [Online] **2018**, 1-26. <https://www.ncbi.nlm.nih.gov/pubmed/29578387> (accessed Feb 1, 2019).
42. InterBioScreen. Databases. 2019. <https://www.ibscreen.com/bases> (accessed Oct 6, 2019).
43. Sterling, T.; Irwin, J. J. Zinc 15-Ligand Discovery for Everyone. *J. Chem. Inf. Model.* **2015**, 55(11), 2324-2337.
44. Cavdar, H.; Senturk, M.; Guney, M.; Durdaqi, S.; Kayik, G.; Supuran, C. T.; Ekinci, D. *J. Enzyme Inhib. Med. Chem.* [Online] **2019**, 34(1), 429-437. <https://www.tandfonline.com/doi/full/10.1080/14756366.2018.1543288> (accessed Oct 6, 2019).
45. Huber, R. J.; O'Day, D. H. *J. Cell. Biochem.* [Online] **2011**, 113: 868-876. <https://www.ncbi.nlm.nih.gov/pubmed/22234985> (accessed Oct 6, 2019).
46. He, D.; Wu, H.; Wei, Y.; Liu, W.; Huang, F.; Shi, H.; Zhang, B.; Wu, Z.; Wang, C. *Eur. J. Pharmacol.* [Online] **2015**, 768, 96-107. <https://www.sciencedirect.com/science/article/pii/S0014299915303174?via%3Dihub> (accessed Oct 6, 2019).
47. Li, R.; Rui, G.; Chen, W.; Li, S.; Schulz, P. E.; Zhang, Y. *Front. Aging Neurosci.* [Online] **2018**, 10, Article 366. <https://www.ncbi>



[nlm.nih.gov/pmc/articles/PMC6237862/pdf/fnagi-10-00366.pdf](https://www.ncbi.nlm.nih.gov/pmc/articles/PMC6237862/pdf/fnagi-10-00366.pdf)  
(accessed Oct 6, 2019).

48. Costanzo, P.; Cariati, L.; Desiderio, D.; Sgammato, R.; Lamberti, A.; Arcone, R.; Salerno, R.; Nardi, M.; Masullo, M.; Oliverio, M. *ACS Med. Chem. Lett.* [Online] **2016**, 7, 470-475. <https://www.ncbi.nlm.nih.gov/pmc/articles/PMC4867475/> (accessed Oct. 6, 2019).

49. Green, K. D.; Fosso, M. Y.; Garneau-Tsodikova, S. *Molecules* [Online] **2018**, 12, 3252. <https://www.ncbi.nlm.nih.gov/pmc/articles/PMC6321525/> (accessed Oct 6, 2019).